Reports

High-Resolution Stratigraphy with Strontium Isotopes

Abstract. *The isotopic ratio of strontium-87 to strontium-86 shows no detectable variation in present-day ocean water but changes slowly over millions of years. The strontium contained in carbonate shells of marine organisms records the ratio of strontium-87 to strontium-86 of the oceans at the time that the shells form. Sedimentary rocks composed of accumulated fossil carbonate shells can be dated and correlated with the use of high precision measurements of the ratio of strontium-87 to strontium-86 with a resolution that is similar to that of other techniques used in age correlation. This method may prove valuable for many geological, paleontological, paleooceanographic, and geochemical problems.*

One of the most important and difficult problems in geology is that of age correlation, particularly the establishment of synchroneity of events on a global scale. We examined the resolution and applicability of measurements of the ratio of ^{87}Sr to ^{86}Sr for correlating ages of Cenozoic marine carbonate-bearing sedimentary rocks. This method appears to be a valuable addition to other stratigraphic correlation tools because it is independent of facies and latitude and may not require the high sample density of paleomagnetic and stable isotopic methods (*1*, *2*).

Burke *et al.* (*3*) determined the strontium isotopic composition of marine precipitates spanning in age the entire Phanerozoic Era. From their data, which were much more precise than those obtained previously (*4*), they were able to reconstruct the history of variations of ^{87}Sr/^{86}Sr in ocean water. They showed that fluctuations of ^{87}Sr/^{86}Sr in seawater occurred more frequently and more abruptly than had been thought (*4*, *5*). Their data show the major trends in the strontium isotopic evolution of seawater and the possibilities for stratigraphic applications.

We sought to make more precise measurements on carefully selected samples to determine the ultimate applicability of strontium isotope stratigraphy and concentrated on samples of Cenozoic age for several reasons. The data of Burke *et al.* (*3*) show that a rapid monotonic increase of ^{87}Sr/^{86}Sr in seawater occurred in the latter part of the Cenozoic. This represents a particularly interesting period for study because of the potential for high-resolution correlation during periods of rapidly changing ^{87}Sr/^{86}Sr. Young sediments also are generally well preserved and provide the best opportunity to calibrate the method against other high-resolution stratigraphic correlation techniques (*6*–*8*). The Cenozoic is also the time period best suited for study of the causes of ^{87}Sr/^{86}Sr variations in ocean water, because there is detailed information on many possible contributory climatic, oceanographic, and tectonic parameters (*9*).

Table 1. Chemical and isotopic data for Holocene samples.

Sample	Description	Location	Sr (ppm)	Rb (ppm)	^{87}Sr/^{86}Sr*
H-2	*Mercenaria mercenaria*	Long Island			0.709234 ± 20
H-3	*Tellina radiata*	Cuba	1494	0.023	0.709256 ± 22
H-4	*Cerastoderma edule*	Great Britain			0.709229 ± 35
H-5	*Turritella communis*	Rimini, Italy	1557	0.87	0.709230 ± 19 0.709237 ± 16
H-1	*Turritella*	Baja California			0.709210 ± 35
H-6	*Cumingia californica*	Southern California	1381	0.123	0.709229 ± 21
H-7	*Dosinia dunkeri*	Sonora, Mexico			0.709241 ± 26
H-8	*Ctena bella*	Hawaii	1357	0.027	0.709229 ± 22 0.709236 ± 12
H-9	*Tellina gaimardi*	New Zealand	1770	0.122	0.709233 ± 26
H-10	*Tellina albinella*	New South Wales, Australia			0.709244 ± 29
H-11	*Nautilus pompilus*	Fiji Islands	2155	0.252	0.709236 ± 30
H-12	*Hippopus hippopus*	Malaysia	1791	0.052	0.709235 ± 36 0.709229 ± 19
H-14	*Bullia debilis*	South Africa			0.709236 ± 20
H-15	*Divaricella divaricata*	Persian Gulf	1670	0.051	0.709232 ± 26
H-16	*Astarte borealis*	Alaska	1450	0.013	0.709228 ± 36

*Normalized to ^{86}Sr/^{88}Sr = 0.1194 to correct for mass discrimination. Analytical uncertainties given represent 2 standard errors of the mean of 200 to 300 individual measurements and refer to the last two digits of the ratio. The ratio measured on NBS 987 standard is 0.71031, so that these ratios are higher than those reported by Burke *et al.* (*3*) by 0.00017.

In order for measurements of ^{87}Sr/^{86}Sr in marine carbonates to be useful for stratigraphic correlation, the ratio in ocean water must be uniform at any time (*10*), the ratio must change sufficiently rapidly with time so that the uncertainty in any measured change is relatively small, and ^{87}Sr/^{86}Sr in carbonate precipitates must not be subsequently modified by diagenesis. We attempted to put limits on the homogeneity of ocean water by measuring modern carbonate shells from all the major oceans (Table 1). The nature and extent of diagenetic alteration in the older samples has not been specifically investigated. Although diagenesis is certainly of general importance, it does not appear to be a problem for the majority of the samples measured in this study, most of which were chosen with the intention of minimizing the potential problems of diagenetic alteration.

The carbonate samples analyzed include, in addition to the modern shells, ooze, and chalk from Deep Sea Drilling Project (DSDP) cores from the Atlantic and Pacific Oceans, fossil molluscs and foraminifera from Oligocene and Eocene strata in the Gulf Coast area of the United States, and whole rock samples from the Oligocene Scaglia Cinerea marlstone in the Contessa Valley, Italy (*11*). Also, molluscan fossils from European localities, including some stage stratotypes, were measured. All but four of the DSDP samples are from sub-bottom depths of less than 150 m. The maximum burial depth of the lowermost sample of the Scaglia Cinerea was about 300 m (*12*). The DSDP sites 522 and 590B are at low latitude, where biostratigraphic control is good and magnetostratigraphy is accurate because hydraulic piston coring was used to obtain undisturbed sediment (*13*). Site 400A is at high latitude, where biostratigraphic control is only fair and drilling deformation prevented detailed magnetostratigraphic studies (*14*).

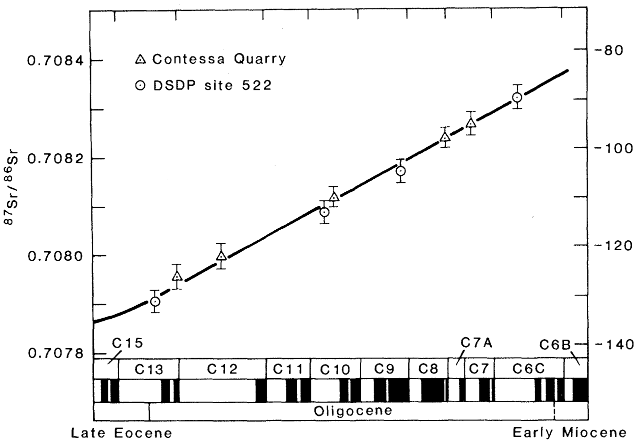

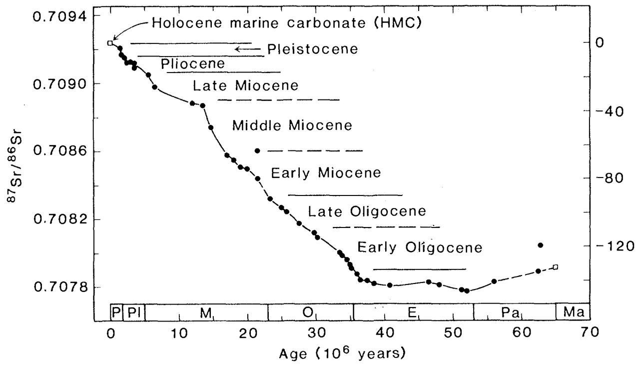

Fig. 1 (left). Measured $^{87}Sr/^{86}Sr$ ratios and $\Delta^{87}Sr$ values of late Eocene and Oligocene chalks and marls plotted as a function of stratigraphic position as determined by magnetic reversals (*11, 20*). Numbers on lower scale designate the paleomagnetic chrons (*6*). The $\Delta^{87}Sr$ parameter is the difference between a measured $^{87}Sr/^{86}Sr$ value and the value for modern carbonates, multiplied by 10^5. Fig. 2 (right). Measured $^{87}Sr/^{86}Sr$ and $\Delta^{87}Sr$ values of Cenozoic marine carbonate samples as a function of age.

Among the fossil shells, many are Scaphopoda; these were chosen because they contain aragonite and consequently high strontium concentrations (*15*), which are indicative of minimal diagenetic alteration. Of the samples in which strontium concentration was measured, all but two have concentrations greater than 1350 ppm.

All the Neogene samples were assigned ages based on biostratigraphic zone assignments and the time scale of Berggren (*7*). The Paleogene samples were assigned ages based on magnetostratigraphy and the time scale of Ness *et al.* (*8*), or based on biostratigraphic zone assignments and the correlations with the magnetostratigraphic scale (*7, 16, 17*).

In order to minimize contamination from noncarbonate materials in the samples, all were dissolved in warm 5 molal acetic acid, and only the soluble fractions were analyzed (*18*). The ratios of ^{87}Rb to ^{86}Sr in all of the samples were less than 0.0012 and are therefore too small for there to be any significant contribution to $^{87}Sr/^{86}Sr$ from decay of ^{87}Rb since the time of deposition. The procedures for mass spectrometric analysis will be detailed elsewhere, but closely follow those described in (*19*).

Measurements of modern shells yielded a mean $^{87}Sr/^{86}Sr$ ratio of 0.709234 with a standard deviation of 0.000009 (Table 1). These data suggest that seawater is extremely uniform in strontium isotopic composition. The small variations we found are well within the statistically estimated 95 percent confidence limits of our individual analyses, and the standard deviation of our 19 measurements is small enough so that it could reflect only the analytical limitations. These data indicate that $^{87}Sr/^{86}Sr$ may be uniform in modern marine carbonates to a level that is below our current resolution. Because different laboratories may measure slightly different values for $^{87}Sr/^{86}Sr$ because of differing instrument characteristics and measurement techniques, we propose the use of a parameter $\Delta^{87}Sr$ (Figs. 1 and 2).

The measurements made on the carbonate fractions of the samples from the Contessa Valley and DSDP site 522 are particularly significant because both sections have been the subject of detailed magnetostratigraphic investigations (*11, 20*). The $^{87}Sr/^{86}Sr$ is plotted against stratigraphic position as determined by paleomagnetic data in Fig. 1. A straight line has been drawn through the data for ease of comparison; it is probable that a more complicated curve would be appropriate, although unjustified by the available data. The agreement of the data from the two sections is remarkable. The average deviation of the data points from the line shown is equivalent to about 2 m in the stratigraphic column or about 0.3 million years (Table 3). These data strongly suggest that diagenesis has not significantly modified the strontium isotope signal in these sediments.

The entire data set is displayed in Fig. 2. A relatively smooth line can be drawn that passes within the analytical uncertainty limits (Table 2) of all but two points, one of which is the sample DSDP

Table 2. Chemical and isotopic data for Pleistocene and Tertiary fossils.

Sample*	Stage	Age† (10^6 years)	Sr (ppm)	Rb (ppm)	$^{87}Sr/^{86}Sr$‡
Ple-5b	Lower Pleistocene	1.5			0.709205 ± 30
Pli-1	Piacenzian	3.5	2753		0.709089 ± 31
M-5	Upper Tortonian	6.5	2273		0.708977 ± 25
M-2	(Choptank Fm.)	12.0	2428	0.47	0.708880 ± 60
M-9	Luisian	13.5			0.708866 ± 33
M-6	Upper Burdigalian	17.0			0.708576 ± 32
Burd-3	Middle Burdigalian	18.0	1779	0.14	0.708547 ± 31
M-7	Middle Burdigalian	18.0			0.708545 ± 27
Burd-2	Lower Burdigalian	19.0	2464	0.20	0.708505 ± 24
A-2	Middle Aquitanian	20.0			0.708493 ± 20
A-1	Basal Aquitanian	21.5			0.708440 ± 23
O-4	Chattian (?)		2829	0.18	0.708283 ± 35
O-3	Vicksburgian	33.8			0.707982 ± 22 0.707963 ± 21
O-7	Vicksburgian	35.0	2856	0.59	0.707928 ± 26
O-8	Lower Stampian				0.708047 ± 24
E-13	Jacksonian	36.0	1350	0.36	0.707874 ± 37
E-5	Jacksonian	37.5	2554	0.43	0.707836 ± 38
E-11	Bartonian	38.5			0.707819 ± 25
E-10	Auversian	40.8			0.707805 ± 23
E-6	Middle Lutetian	46.4	2003	0.02	0.707823 ± 34
E-1	Claiborne	48.0			0.707808 ± 27
E-2	Cuisian	51.2	3444	0.01	0.707778 ± 22
E-4	Wilcox	52.0			0.707772 ± 27
P-2	Thanetian	56.0			0.707826 ± 26
P-3	Middle Danian	62.8			0.708043 ± 40

*Samples are described in (*30*). †Samples for which no age is given are not plotted in Fig. 2. ‡See explanation in Table 1.

Table 3. Chemical and isotopic data for acetic acid soluble fractions of chalks and marls.

Location	Sample*	Age (10^6 years)	$CaCO_3$† (%)	Sr (ppm)	Rb (ppm)	$^{87}Sr/^{86}Sr$‡
DSDP Leg 90, site 590B, Tasman Sea	Core 4-6 (30 m)	1.7	99	1476	0.53	0.709162 ± 17
	core 5-6 (39 m)	1.9	99	1763	0.55	0.709156 ± 14
	core 6-3 (44 m)	2.4	99	1912	0.50	0.709125 ± 17
	core 8-6 (68 m)	2.7	99	1892	0.42	0.709129 ± 21
	core 12-6 (107 m)	3.5	99	1780	0.75	0.709113 ± 32
DSDP Leg 48, site 400A, North Atlantic	Core 20-3 (259 m)	5.5	69	1806	0.42	0.709051 ± 34
						0.709050 ± 30
	core 31-1 (360 m)	14.7	71	1929	0.41	0.708736 ± 31
	core 40-2 (448 m)	21 ?	59	2115	0.55	0.708593 ± 25
DSDP Leg 73, site 522, South Atlantic	Core 15-2 (57 m)	23.3	82	1655	0.40	0.708320 ± 24
	core 20-2 (79 m)	27.6	83	2064	0.22	0.708172 ± 24
	core 25-2 (93 m)	30.2	91	1527	0.22	0.708088 ± 22
	core 35-2 (134 m)	35.2	93	1464	0.14	0.707908 ± 25
Contessa Quarry, Gubbio, Italy	298.00 m	25.0	62	2709	1.17	0.708268 ± 27
	292.35 m	25.7				0.708240 ± 21
	269.45 m	29.8				0.708119 ± 20
	241.80 m	33.4				0.707999 ± 28
	232.40 m	34.6	74	1571	0.52	0.707958 ± 28
	211.80 m	36.5	82			0.707838 ± 21
DSDP Leg 17, site 167, Pacific	Core 39-1	62 to 63		1125		0.707886 ± 21
DSDP Leg 62, site 465A, Pacific	Core 3-3 (62 m)	65	99	1264	0.28	0.707916 ± 36
	core 3-4 (63 m)	65	90	707	0.73	0.707906 ± 36
	core 3-4 (63 m)	65	99	1249	0.60	0.707914 ± 34

*For DSDP samples, the numbers following the core number represent the section number and the sub-bottom depth. Contessa Quarry samples are described in (*11*). For DSDP site 522 and Contessa Quarry, ages were assigned on the basis of paleomagnetic reversal stratigraphy (*11, 20*) and the time scale recommended by Ness *et al.* (*8*). †Numbers given represent percent of sample soluble in 5 molal acetic acid. ‡See explanation in Table 1.

400A-40 (early Miocene age). There is reason to regard this sample as anomalous because the other six early Miocene samples describe a smooth curve and are perfectly consistent with the stratigraphic succession. Although there are uncertainties with regard to the age assignment of this sample (*21*), this relatively deeply buried sediment may have undergone strontium isotopic modification during diagenesis. This suggestion is based on the results of studies of strontium concentration in deep-sea carbonates and interstitial waters (*22*) which show that the effects of diagenesis become pronounced in sediments buried to depths greater than 300 to 400 m. The other problematic point is of early Paleocene age; additional data are required to resolve the discrepancy.

The new data generally agree with those of Burke *et al.* (*3*) but show significantly less scatter. With regard to the rate of change of $^{87}Sr/^{86}Sr$, the curve can be divided into two parts. Between the Cretaceous-Tertiary boundary and the late Eocene, $^{87}Sr/^{86}Sr$ generally decreases and shows minor fluctuations, whereas from the latest Eocene to the present it has been increasing rapidly. Provided that there are no major problems with age assignments, the data further suggest that there were significant variations in the rate of increase (*23*) of seawater $^{87}Sr/^{86}Sr$ since the late Eocene and that these small variations and the larger-scale variations are correlated with the temperature of oceanic bottom waters as reflected in the oxygen isotopic composition of benthic foraminifera (*24*) and with other paleoceanographic and paleoclimatic indicators (Fig. 3). Periods of particularly rapid growth of marine $^{87}Sr/^{86}Sr$ occurred near the Eocene-Oligocene boundary, in the early middle Miocene and in the late Pliocene to the Pleistocene (*25*). Extended periods of increase of $^{87}Sr/^{86}Sr$ are correlated with decreasing bottom-water temperature, increased carbonate compensation depth, lower continental temperatures, and lower sea level (*26*–*28*). Especially rapid increases are contemporaneous with the onset of glaciations or the formation of polar sea ice (*9*).

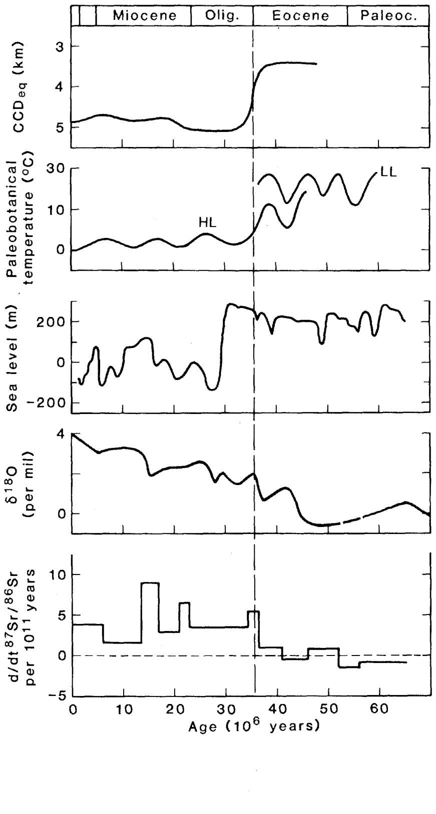

Fig. 3. Comparison of the rate of change of marine $^{87}Sr/^{86}Sr$ (from Fig. 2) and other paleoclimatic and paleoceanographic data. CCD_{eq} is the carbonate compensation depth in the equatorial Pacific (*26*); HL and LL stand for high and low latitudes, respectively (*27*). The absolute value of the fluctuations in sea level are approximate; 0 represents the present-day sea level (*28*). The $\delta^{18}O$ curve is generalized from (*23*).

With regard to stratigraphic correlation problems, notable results of our measurements are the large difference in $^{87}Sr/^{86}Sr$ between the sample from a basal Aquitanian stratum (A-1) and DSDP 522-15-2 (*Globigerinoides* datum) (*25*) and the high $^{87}Sr/^{86}Sr$ of the Chattian sample (*29*). Also, the strontium isotope succession in the Gulf Coast region of the United States (Table 2) agrees well with those of the Contessa section and DSDP site 522, as does the analysis of a Stampian sample from the Paris Basin (*16, 29*).

DONALD J. DEPAOLO
BONNYE L. INGRAM
Department of Earth and Space Sciences, University of California, Los Angeles 90024

References and Notes

1. N. D. Watkins, *Geol. Soc. Am. Bull.* **83**, 551 (1972); A. Cox, R. R. Doell, G. B. Dalrymple, *Science* **144**, 1537 (1964).
2. C. Emiliani, *J. Geol.* **66**, 264 (1958).
3. W. A. Burke, R. E. Denison, E. A. Hetherington, R. B. Koepnik, H. F. Nelson, J. B. Otto, *Geology* **10**, 516 (1982).
4. Z. E. Peterman, C. E. Hedge, H. A. Tourtelot, *Geochim. Cosmochim. Acta* **34**, 105 (1970); E. J. Dasch and P. E. Biscaye, *Earth Planet. Sci. Lett.* **11**, 201 (1971); G. Faure, P. M. Hurley, J. L. Powell, *Geochim. Cosmochim. Acta* **29**, 209 (1965); J. Kovach and G. Faure, *N.Z. J. Geol. Geophys.* **20**, 1017 (1977); E. L. Tremba, G. Faure, G. C. Katsikatsos, C. H. Summerson, *Chem. Geol.* **16**, 109 (1975); V. R. Murthy and E. Beiser, *Geochim. Cosmochim. Acta* **32**, 1121 (1968); E. I. Hamilton, *Earth Planet. Sci. Lett.* **1**, 435 (1966).
5. G. W. Brass, *Geochim. Cosmochim. Acta* **40**, 721 (1976); J. Veizer and W. Compston, *ibid.* **38**, 1461 (1974).
6. W. B. Harland *et al.*, *A Geologic Time Scale* (Cambridge Univ. Press. Cambridge, England, 1982).
7. W. A. Berggren, *Lethaia* **5**, 195 (1972).
8. G. Ness, S. Levi, R. Couch, *Rev. Geophys. Space Phys.* **18**, 753 (1980).
9. J. P. Kennett, *Marine Geology* (Prentice-Hall, Englewood Cliffs, N.J., 1982); *J. Geophys. Res.* **82**, 3843 (1977).
10. The isotopic homogeneity of strontium in the oceans is related to the ratio of the residence time of strontium in the oceans. τ, to the mixing time of the oceans, τ_m. For strontium, $\tau/\tau_m = 4000$, so that a high degree of homogeneity is expected [W. S. Broecker, in *The Sea*, M. N. Hill, Ed. (Interscience, New York, 1963), vol. 2, pp. 88–108; E. D. Goldberg, in *ibid.*, p. 3; H. D. Holland, *The Chemistry of the Atmosphere and Oceans* (Wiley, New York, 1978), chap. 1.
11. W. Lowrie, W. A. Alvarez, G. Napoleon, K. Perch-Nielsen, I. Premoli-Silva, M. Tourmarkine, *Geol. Soc. Am. Bull.* **93**, 414 (1982).
12. M. Orlando, stratigraphic column presented at the International Geological Correlation Program meeting (Project 174) (Gubbio, Italy, April 1984).
13. *Init. Rept. Deep Sea Drill. Proj.* **73** (1983).
14. *Init. Rept. Deep Sea Drill. Proj.* **48** (1979).
15. Aragonite formed in equilibrium with ocean water would have about 8700 ppm strontium whereas calcite would have 1050 ppm [D. J. Kinsman, *J. Sediment. Petrol.* **39**, 486 (1969)]. Most shells have higher concentrations resulting from biogenetic effects [H. A. Lowenstam, *J. Geol.* **69**, 241 (1961)].
16. D. Curry and G. S. Odin, in *Numerical Dating in Stratigraphy*, G. S. Odin, Ed. (Wiley, New York, 1981), p. 607.
17. There are sizeable uncertainties associated with the absolute values of assigned ages, but it is not possible to specify the uncertainty precisely because the relative ages are constrained by stratigraphic succession. The age of any single sample cannot generally be changed without simultaneously modifying the ages of other samples in the same age range, that is, modifying the time scale (*7*).
18. Whole rock samples were dried (DSDP samples) or crushed (Contessa Quarry samples) and placed in 5 molal acetic acid in an ultrasonic bath for 1 hour. Fossil samples were cleaned of sediment in an ultrasonic bath with distilled water, crushed, and then likewise dissolved in acetic acid. The dissolved samples were centrifuged, the liquid was pipetted off, evaporated to dryness, and the residue redissolved in $1.5N$ hydrochloric acid. Standard ion-exchange techniques were used to separate strontium for mass spectrometric analysis. Detailed procedures are described by D. J. DePaolo, F. T. Kyte, B. D. Marshall, J. R. O'Neil, and J. Smit [*Earth Planet. Sci. Lett.* **64**, 356 (1983)].
19. D. J. DePaolo, *J. Geophys. Res.* **86**, 10470 (1981); in preparation.
20. R. Z. Poore, L. Tauxe, S. F. Percival, J. L. LaBreque, *Geology* **10**, 508 (1982).
21. C. A. Muller, *Init. Rept. Deep Sea Drill. Proj.* **48**, 589 (1979); V. A. Krashininnikov, *ibid.*, p. 431.
22. P. A. Baker, J. M. Gieskes, H. Elderfield, *J. Sediment. Petrol.* **52**, 71 (1982); H. Elderfield and J. M. Gieskes, *Nature (London)* **300**, 493 (1982).
23. If $^{87}\text{Sr}/^{86}\text{Sr}$ in the oceans is denoted R_o, and $^{87}\text{Sr}/^{86}\text{Sr}$ of the strontium being continuously added to the oceans by rivers and other sources is denoted R_i, then the rate of change (R'_o is given by $R'_o = \tau^{-1}(R_i - R_o)$ [*5*; F. Albarede, A. Michard, J. F. Minster, G. Michard, *Earth Planet. Sci. Lett.* **55**, 229 (1981)]; R_o responds to changes of R_i with a charactertistic response time equal to τ (~4 million years) (*10*).
24. S. M. Savin, R. G. Douglas, F. G. Stehli, *Geol. Soc. Am. Bull.* **86**, 1499 (1975).
25. The apparent rapid increase near the Oligocene-Miocene boundary is questionable, as there are relatively large uncertainties in the age assignments for the early Miocene samples [M. S. Srinivasan and J. P. Kennett, *Mar. Micropaleo.* **6**, 499 (1981)].
26. T. H. van Andel, G. R. Heath, T. C. Moore, *Geol. Soc. Am. Mem. 143* (1975).
27. J. A. Wolfe, *Am. Sci.* **66**, 694 (1978).
28. P. R. Vail, R. M. Mitchum, R. G. Todd, J. M. Widmier, S. Thompson, J. B. Sangree, J. N. Bubb, W. G. Hatlelid, *Am. Assoc. Petrol. Geol. Mem. 26*, (1977), p. 49.
29. W. A. Berggren, D. V. Kent, J. J. Flynn, *Geol. Soc. Lon. Spec. Pap.*, in press.
30. Ple-5b: *Cardita (Cyclocardita) occidentalis*, lower member of the Santa Barbara Formation (Fm), Bathhouse Beach, Packard Hill, Santa Barbara, Calif. Pli-1: Scaphopoda, east side of Lago d'Argano, Arignano, Italy (Piacenzian type area). M-5: Scaphopoda, Upper Tortonian marls, east of Santa Agato and northwest of Bavautore; type locality and type fauna. M-2: *Cadulus newtonensis*, Choptank Fm, Calvert Cliffs, west shore of Chesapeake Bay, Md. M-9: *Valvulinaria californica*, Luisian marl, Monterey Fm, Orange County, Calif. M-6: Scaphopoda, Saucats, 21 km nearly due south of the center of Bordeaux, Gironde, France. Burd-3: *Oxystele burdigalensis*, Léognan, Gironde, France (Burdigalian type area). M-7: *Dentalium (Antalis) exlamarki*, Léognan, Gironde, France. Burd-2: *Nuculana (Lembulus) emarginata*, Le Thibaudeau, Léognan, France. A-2: *Timoclea subspadicea*, Lariey, near Saucats, France. A-1: *Corbulomya (Lentidium) tournoueri*, Le Brède, France. O-4: *Dentalium*, Trift, near Weinheim, 18 km west of Mainz, Germany. O-3: *Dentalium*, Byram marl, roadcut on Highway 61, 5 km north of the gate of the Vicksburg National Cemetary, Vicksburg, Miss. O-7: *Dentalium*, Mint Spring marl at Spring Bayou, just south of National Cemetary entrance, 750 m east of Highway 61, Vicksburg, Miss. (basal Vicksburg Group). O-8: Pelycypod fragment, Morigny, France (zone of Morigny). E-13: *Hantkenina*, Pachuta member, Yazoo Fm, Clarke County, Miss. E-11: *Dentalium striatum*, Barton, Hants, England (Bartonian type area). E-10: *Dentalium*, Auvers, France (Auversian type area). E-5: Scaphopoda, Moodys marl member of Jackson Fm, Hinds Co., Miss. E-1: *Dentalium (Antalis) thalloides*, Lisbon Fm, Claiborne, Alabama. E-6: *Cardita*, Paris Basin, Damerey, France, overlying Ypresian clay sand (middle Lutetian zone III). E-2: *Dentalium (Fustiaria) lucidum*, Monampteuil, France. E-4: *Cadulus abruptus*, Tuscahoma Fm, Wilcox Group, Bell's Landing, east bank of Alabama River, Monroe County, Alabama. P-2: *Diplodonta laevigata*, Châlons sur Vesle, Marne, France. P-3: *'Rhynchonella' flustracea*, Faxe, Zealand, Denmark (Danian type area).
31. We thank L. Saul, L. W. Alvarez, H. Loeblich, A. Loeblich, and the Deep Sea Drilling Project for providing samples. Supported by a grant from the donors of the Petroleum Research Fund, administered by the American Chemical Society, and NSF grant EAR 82-66092.

18 June 1984; accepted 26 October 1984

Chromosomal Locations of the Murine T-Cell Receptor Alpha-Chain Gene and the T-Cell Gamma Gene

Abstract. *Two independent methods were used to identify the mouse chromosomes on which are located two families of immunoglobulin (Ig)-like genes that are rearranged and expressed in T lymphocytes. The genes coding for the* α *subunit of T-cell receptors are on chromosome 14 and the gamma genes, whose function is yet to be determined, are on chromosome 13. Since genes for the T-cell receptor* β *chain were previously shown to be on mouse chromosome 6, all three of the Ig-like multigene families expressed and rearranged in T cells are located on different chromosomes, just as are the B-cell multigene families for the Ig heavy chain, and the Ig kappa and lambda light chains. The findings do not support earlier contentions that genes for T-cell receptors are linked to the Ig heavy chain locus (mouse chromosome 12) or to the major histocompatibility complex (mouse chromosome 17).*

Recent studies have revealed similarities and differences between the antigen-specific receptors of the B- and T-lymphocyte populations, which, together, make up the bulk of the cells of the immune system. The receptors on B cells have long been known to be immunoglobulins (Ig). Those on T cells consist of Ig-like integral membrane glycoproteins containing two polypeptide subunits (α and β) of similar molecular weight, 40 to 45 kD in the mouse (*1, 2*) and 40 to 55 kD in the human (*3*). Like Ig's on B cells, each T-cell receptor subunit has, external to the cell membrane, an amino terminal variable domain (V) and a carboxyl terminal constant (C) domain (*4–6*). The genes that encode these subunits have been identified (*7–13*) and, like Ig genes, are assembled from gene segments (*14–18*). There are at least four segments for β chains—variable (V), diversity (D), joining (J), and constant (C)—and three, so far, for α chains (V, J, and C).

During the search for the T-cell receptor genes, Saito *et al.* (*11, 19*) identified in T lymphocytes another Ig-like gene, called γ. Like the α and β genes, the γ gene is also assembled in T cells (but not in B cells) from gene segments that are homologous to the Ig V, J, and C segments. The function of the γ gene is not known, but the fact that it is assembled from gene segments in T cells (*20*) and shows clonal diversity in V region sequences (*21*) suggests that its product is (or is part of) a second T-cell receptor that helps determine T-cell specificity. The possibility that there are two receptors on T cells, rather than one, has long been debated, because of a difference in the way B and T cells recognize antigens: B cells (like antibody molecules)